HHS Public Access

Author manuscript

Angew Chem Int Ed Engl. Author manuscript; available in PMC 2022 March 09.

Published in final edited form as:

Angew Chem Int Ed Engl. 2019 September 23; 58(39): 13865–13868. doi:10.1002/anie.201906005.

Insertion of CO_2 Mediated by a (Xantphos)Ni^{I}–Alkyl Species

Justin B. Diccianni, **Chunhua T. Hu**, **Tianning Diao**[*] **[Assist. Prof.]**

Chemistry Department, New York University, 100 Washington Square East, New York, NY 10003 (USA)

Abstract

The incorporation of CO_2 into organometallic and organic molecules represents a sustainable way to prepare carboxylates. The mechanism of reductive carboxylation of alkyl halides has been proposed to proceed through the reduction of Ni^{II} to Ni^{I} by either Zn or Mn, followed by CO_2 insertion into Ni^{I}-alkyl species. No experimental evidence has been previously established to support the two proposed steps. Demonstrated herein is that the direct reduction of (tBuXantphos)$Ni^{II}Br_2$ by Zn affords Ni^{I} species. (*t*Bu-Xantphos)-Ni^{I}-Me and (*t*Bu-Xantphos)Ni^{I}-Et complexes undergo fast insertion of CO_2 at 22°C. The substantially faster rate, relative to that of Ni^{II} complexes, serves as the long-sought-after experimental support for the proposed mechanisms of Ni-catalyzed carboxylation reactions.

Keywords

carbon dioxide; nickel; reaction mechanisms; reduction; structure elucidation

Carbon dioxide (CO_2) is a sustainable, inexpensive, and clean C1 source for chemical synthesis.[1] These advantages underlie recent advances in developing Ni-catalyzed reactions to incorporate CO_2 into organic molecules.[2] Dong and co-workers reported the Ni-catalyzed carboxylation of organozinc reagents, giving rise to a variety of carboxylic acids.[3] Applying reductive conditions, the groups of Rovis,[4] Martin,[5] Tsuji,[6] and others[2] expanded the scope of carboxylation substrates to alkenes, aryl halides, and alkyl halides. The carboxylation of alkyl halides is proposed to initiate with the oxidative addition of Ni^{0} into an alkyl bromide, followed by the reduction of the Ni^{II} intermediate by either Mn or Zn to give a Ni^{I}-alkyl species (Scheme 1).[5a,b] Carboxylation of the Ni^{I}-alkyl intermediate gives rise to the carboxylate product. Computational studies on the reductive carboxylation of chlorobenzene suggest a similar mechanism, where a Ni^{I}-phenyl intermediate is responsible for carboxylation.[7] The reduction of Ni^{II} to Ni^{I} by either Mn or Zn and CO_2 insertion into Ni^{I}-alkyl intermediates have not been established before. In light of the rapid growth of Ni-catalyzed carboxylation to harness CO_2 as a chemical source, it is critical to obtain evidence for the proposed mechanism to inform future catalyst design.

[*] diao@nyu.edu .

Supporting information and the ORCID identification number(s) for the author(s) of this article can be found under: https://doi.org/10.1002/anie.201906005.

Conflict of interest

The authors declare no conflict of interest.

The insertion of CO_2 into organometallic molecules has been a long-time pursuit of fundamental studies.[8] While CO_2 insertion into Ni^{II}-H complexes proved to be facile,[9] only three examples of CO_2 insertion into Ni-carbyl complexes have been reported.[10] PCP-pincer-ligand-stabilized Ni^{II}-Me molecules undergo slow CO_2 insertion at 150°C [Eq. (1)]. The

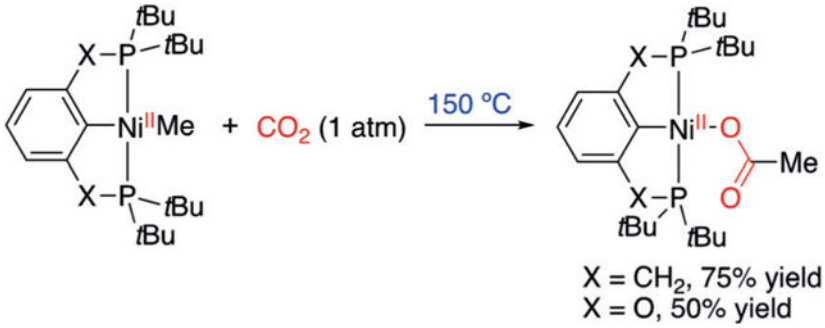

low reactivity contradicts the facile catalytic reactivity that has emerged in recent literature.[2] Computational studies predict that the more electron-rich Ni^{I}-carbyl complex undergoes faster CO_2 insertion than Ni^{II}-carbyl complexes, as the carboxylation is nucleophilic in nature.[7] This hypothesis has found support in the recent observation of CO_2 insertion into a Ni^{I}-aryl complex at room temperature.[10c] The Ni carboxylate product, however, was not characterized. The scarcity of examples of CO_2 insertion into Ni^{I}-carbyl complexes is likely due to the difficulty of isolating well-defined Ni^{I}-carbyl and carboxylate molecules.[11,12] The previous Ni^{I}-alkyl[13] and Ni^{I}aryl[14] complexes have exceedingly bulky ligands to stabilize the open-shell molecules, and this is likely detrimental toward their reactivity with CO_2.[14b,15] In light of the catalytic significance of Ni^{I}-carbyl complexes in mediating CO_2 insertion and the fundamental interest in this bond-formation process, herein, we report the chemical reduction of Ni^{II} complexes to Ni^{I} and the first example of insertion of CO_2 into Ni^{I}-alkyl complexes. This work serves as experimental support for the proposed mechanisms involving Ni^{I} species in Ni-catalyzed carboxylation reactions.

Bulky bidentate ligands with large bite angles can stabilize Ni^{I} complexes.[14b,15] We have recently demonstrated this concept in preparing (*t*Bu-Xantphos)Ni^{I}Ar complexes.[16] In an effort to prepare Ni^{I}-alkyl complexes, we treated (*t*BuXantphos)$Ni^{II}Br_2$ (**1**) with Zn in THF to generate a canary yellow solution (Scheme 2). X-ray crystallography established the product to be a 1:1 mixture of the $ZnBr_2$-bound (*t*BuXantphos)Ni^{I}Br (**2**) and (*t*Bu-Xantphos)Ni^{I}Br (**3;** see Figure S2 in the Supporting Information). The ^{1}H NMR spectrum shows that no **3** is present in solution, indicating that the major species is **2**. This single-electron reduction of Ni^{II} zinc supports a proposed intermediate step in catalytic carboxylation reactions (Scheme 1).[5a,b] Clean **3**, without ZnBr2, can be obtained in high yields by the reduction of **1** with Cp_2Co (Scheme 2). The EPR spectrum of **3** shows coupling to the bromide atom and both phosphines from the (*t*Bu-Xantphos) ligand (see Figure S24).

Alkylation of **3** with MeLi and EtLi afforded (*t*Bu-Xantphos)NiMe **(4)** and (*t*Bu-Xantphos)NiEt **(5)**, respectively, as dark brown solids (Scheme 2). The low yield of **5**

is attributed to fast decomposition, likely by b-hydride elimination, followed by ejection of a hydrogen radical to form (*t*Bu-Xantphos)Ni(N_2).[16] Attempts to use a Ph-Xantphos ligand resulted in rapid decomposition. The crystal structure of **4** shows a slightly distorted trigonal-planar geometry, with the O-atom of *t*Bu-Xantphos weakly interacting with Ni (Ni(1)–O(1)=2.6018(11) Å; Figure 1A). The Ni-C(1) bond length of 2.055(7) Å is longer than that of (terpy)NiMe (1.95(13) Å),[13a] and may be related to the redox activity of the terpy ligand. The structure of **5** is similar to that of **4**, with a long β-H—Ni distance (3.18 c), suggesting the lack of a bagostic interaction (Figure 1B).[17] Addition of lithium acetylide reagents to **3** generated the Ni^{I}-acetylides **6** and **7**. The crystal structure of **6** shows a Ni(1)-C(1)-C(2) angle of 174.53(14)°, consistent with an sp-hybridized C(1) (Figure 1C). The decreasing Ni(1)-C(1) bond lengths of **4**, **5**, **11**,[16] and **6** reveal increasing bond strengths on the order of sp^3 <sp^2 <sp (Table 1). The spin-density plots of **4**–**6** obtained by DFT calculations reveal that the unpaired electron is primarily localized on the Ni center, with a small portion distributed to C(1) (Figure 1).[18] The spin-density is higher on C(1) for **4** and **5** than for **6** and **11**, suggesting that the carbyl fragments on the former compounds have a more significant radical character. The EPR spectra of both **4** and **11** show strong coupling to the two phosphorus atoms of the (*t*Bu- Xantphos) ligand and minimal coupling to the protons on the carbyl fragments (see Figures S25 and S26).

Introducing 1 atm of CO_2 to **4** immediately generated the Ni^{I}-carboxylate **9** as an orange compound [Eq. (2)]. The structure of **9** exhibits a trigonal-planar geometry with a secondary interaction between Ni and the Xantphos O(1) with a distance of 2.471 Å (Figure 2). The Ni-O(2) distance of 2.0145(13) Å is noticeably longer than that of the previously reported (PNP)Ni^{II}-formate (1.927(5) Å).[10a] The longer NiO(2) distance reflects a more electron-rich Ni center. The long distance of 2.9003(17) Å between Ni and O(3) reveals

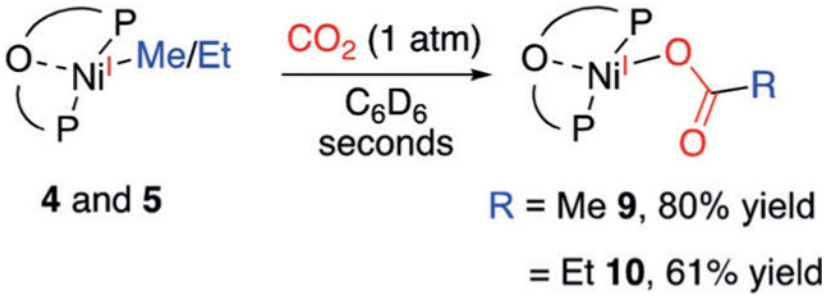

that the acetate is coordinated in an η^1 fashion. The EPR spectrum of **9** shows that the unpaired electron is coupled to phosphorus atoms of the (*t*Bu-Xantphos) ligand and possibly to the protons on the acetate group (see Figure S26). The reaction of **5** with CO_2 afforded **10** in 61% yield, as characterized by its analogous ^{1}H NMR spectrum to that of **9**. It is noteworthy that the carboxylation reactions are quite rapid, finishing in seconds at room temperature. This fast rate contrasts with those observed for (PCP)Ni^{II}-Me,[10] and is corroborated by previous DFT calculations.[7]

The other (*t*Bu-Xantphos)Ni^{I} molecules **6**, **7**, **8**, and **11**, however, did not react with CO_2 over 24 hours under either 1 atm or 4 atm of CO_2 (Scheme 3). Addition of Lewis acids,

including LiCl, $LiBF_4$, BPh_3, and $ZnCl_2$ did not promote CO_2 insertion.[10c] When the less bulky (Ph-Xantphos)Ni^{I}Ph is formed in situ from the reaction of (Ph-Xantphos)Ni^{II}BrPh and Zn under one atmosphere of CO_2, benzoic acid is obtained in 48% yield (see page S8 in the Supporting Information). This result suggests that the greater Ni–Csp^2 bond strength, relative to the Ni–Csp^3 bond, is not the factor that hinders carboxylation of **11**. Instead, we attribute the contrasting reactivity of Ni-alkyls with Ni-aryls/alkynyls to their different mechanisms of insertion (Scheme 4). Ni^{I}-alkyl complexes could undergo insertion by nucleophilic attack of the alkyl groups to CO_2, as proposed in previous computational studies (Scheme 4A).[10a] In contrast, sp and sp^2 nucleophiles cannot access such a pathway, but can only undergo migratory insertion (Scheme 4B). The approach of CO_2 to these (*t*Bu-Xantphos)Ni^{I} complexes is inhibited by the bulky substituents on the ligand.[8c] The lack of reactivity of **8** with CO_2 can be attributed to the lower nucleophilicity of phenoxides compared with carbanions.

Finally, to verify the catalytic relevance of (Xantphos)Ni complexes, we tested the catalytic carboxylation of BnZnCl, PhZnCl, and n-BuZnCl, as well as the reductive carboxylation of benzyl bromide.[3] Either with no ligand or with *t*Bu-Xantphos, no carboxylation reaction took place for zinc reagents, as the *t*Bu-Xantphos ligand stabilizes Ni^{I} species and does not allow catalytic turnover. The use of Ph-Xantphos led to carboxylation of all three organozinc reagents under mild reaction conditions to afford the corresponding benzylacetic, benzoic, and valeric acids (Scheme 5A). (Ph-Xantphos)$Ni^{II}Br_2$ could be reduced in situ to Ni^{I} and, in fact, (PhXantphos)Ni^{I}Br renders a better yield for the carboxylation of *n*-BuZnCl. The catalytic reactivity of PhZnCl contrasts with the lack of stoichiometric reactivity of **11**, but is consistent with the reactivity of in situ formed (Ph-Xantphos)Ni^{I}Ph (see page S8), highlighting the access to the migratory insertion pathway that comes with a smaller steric profile (Scheme 4B). (Ph-Xantphos)$Ni^{II}Br_2$ also catalyzes reductive carboxylation of BnBr, albeit in low yield, but the bulkier (*t*Bu-Xantphos)Ni^{I}Br does not effectively turn over the reaction (Scheme 5B).

In summary, the direct reduction of (*t*Bu-Xantphos)$Ni^{II}Br_2$ by Zn generates (*t*Bu-Xantphos)Ni^{I}Br. (*t*Bu-Xant-phos)Ni^{I}-Me and (*t*Bu-Xantphos)Ni^{I}-Et complexes undergo fast insertion of CO_2 at 228C, whereas (*t*Bu-Xantphos)Ni^{I}phenyl, acetylide, and phenoxide complexes gave no insertion products. This observation represents the first characterization of CO_2 insertion into Ni^{I}–alkyl bonds and verifies the nucleophilic addition mechanism proposed by previous DFT calculations. The fast reaction rate corroborates the facile catalytic reactions and the predicted importance of Ni^{I} intermediates relative to Ni^{II} in carboxylation. Characterization of these stoichiometric reactions provides evidence to support mechanistic proposals for Ni-catalyzed carboxylation reactions of organic and organometallic reagents.

Supplementary Material

Refer to Web version on PubMed Central for supplementary material.

Acknowledgements

J.D. thanks Paul Peterson and John Eng (Princeton University) for assistance with the EPR measurements and Qiao Lin for simulating the EPR spectra. This work was supported by the National Science Foundation under Award Number CHE-1654483. J.D. is supported by the Margaret and Herman Sokol Fellowship and the Ted Keusseff Fellowship. T.D. is a recipient of the Alfred P. Sloan Research Fellowship (FG-2018-10354) and the Camille-Dreyfus Teacher-Scholar Award (TC-19-019). T.D. acknowledges NSF (CHE-1827902) for funding to acquire an EPR spectrometer.

References

[1]. a)Behr A, Angew. Chem. Int. Ed. Engl 1988, 27, 661–678; Angew. Chem. 1988, 100, 681–698;b)Aresta M, Carbon Dioxide as Chemical Feedstock, Wiley-VCH, Weinheim, 2010;c)Aresta M, Dibenedetto A, Quaranta E, Catal J. 2016, 343, 2–45.

[2]. For reviews, see: a)Sakakura T, Choi J-C, Yasuda H, Chem. Rev 2007, 107, 2365–2387; [PubMed: 17564481] b)Correa A, Martín R, Angew. Chem. Int. Ed 2009, 48, 6201–6204; Angew. Chem. 2009, 121, 6317–6320;c)Martín R, Kleij AW, ChemSusChem 2011, 4, 1259–1263; [PubMed: 21567978] d)Huang K, Sun C-L, Shi Z-J, Chem. Soc. Rev 2011, 40, 2435–2452; [PubMed: 21387036] e)Cokoja M, Bruckmeier C, Rieger B, Herrmann WA, Kghn FE, Angew. Chem. Int. Ed 2011, 50, 8510–8537; Angew. Chem. 2011, 123, 8662–8690;f)Tsuji Y, Fujihara T, Chem. Commun 2012, 48, 9956–9964;g)Zhang L, Hou Z, Chem. Sci 2013, 4, 3395–3403;h)Yeung CS, Dong VM, Top. Catal 2014, 57, 1342–1350;i)Liu Q, Wu L, Jackstell R, Beller M, Nat. Commun 2015, 6;j)Yu B, He L-N, ChemSusChem 2015, 8, 52–62; [PubMed: 25209543] k)Bçrjesson M, Moragas T, Gallego D, Martin R, ACS Catal. 2016, 6, 6739–6749; [PubMed: 27747133] l)Juliá-Hernández F, Gaydou M, Serrano E, van Gemmeren M, Martin R, Top. Curr. Chem 2016, 374, 1–38;m)Li Y, Cui X, Dong K, Junge K, Beller M, ACS Catal. 2016, 6, 1077–1086;n)Fujihara T, Tsuji Y, J. Jpn. Pet. Inst 2016, 59, 84–92;o)Zhang L, Hou Z, Curr. Opin. Green Sustainable Chem 2017, 3, 17–21;p)Tortajada A, Juliá-Hernández F, Börjesson M, Moragas T, Martin R, Angew. Chem. Int. Ed 2018, 57, 15948–15982; Angew. Chem. 2018, 130, 16178–16214.

[3]. Yeung CS, Dong VM, J. Am. Chem. Soc 2008, 130, 7826–7827. [PubMed: 18510323]

[4]. Williams CM, Johnson JB, Rovis T, J. Am. Chem. Soc 2008, 130, 14936–14937. [PubMed: 18928253]

[5]. a)Correa A, Martán R, J. Am. Chem. Soc 2009, 131, 15974– 15975; [PubMed: 19886688] b)León T, Correa A, Martin R, J. Am. Chem. Soc 2013, 135, 1221–1224; [PubMed: 23301781] c)Liu Y, Cornella J, Martin R, J. Am. Chem. Soc 2014, 136, 11212–11215; [PubMed: 25068174] d)Moragas T, Cornella J, Martin R, J. Am. Chem. Soc 2014, 136, 17702–17705; [PubMed: 25473825] e)Wang X, Nakajima M, Martin R, J. Am. Chem. Soc 2015, 137, 8924–8927. [PubMed: 26130587]

[6]. Fujihara T, Nogi K, Xu T, Terao J, Tsuji Y, J. Am. Chem. Soc 2012, 134, 9106–9109. [PubMed: 22612592]

[7]. Sayyed FB, Tsuji Y, Sakaki S, Chem. Commun 2013, 49, 10715–10717.

[8]. a)Fan T, Chen X, Lin Z, Chem. Commun 2012, 48, 10808– 10828;b)Hazari N, Heimann JE, Inorg. Chem 2017, 56, 13655–13678; [PubMed: 29115825] c)Obst M, Pavlovic L, Hopmann KH, J. Organomet. Chem 2018, 864, 115–127.

[9]. Darensbourg DJ, Darensbourg MY, Goh LY, Ludvig M, Wiegreffe P, J. Am. Chem. Soc 1987, 109, 7539–7540.

[10]. a)Schmeier TJ, Hazari N, Incarvito CD, Raskatov JA, Chem. Commun 2011, 47, 1824–1826;b)Jonasson KJ, Wendt OF, Chem. Eur. J 2014, 20, 11894–11902; [PubMed: 25080339] c)Charboneau DJ, Brudvig GW, Hazari N, Lant HMC, Saydjari AK, ACS Catal. 2019, 9, 3228–3241. [PubMed: 31007967]

[11]. Horn B, Limberg C, Herwig C, Braun B, Chem. Commun 2013, 49, 10923–10925.

[12]. a)Lin C-Y, Power PP, Chem. Soc. Rev 2017, 46, 5347–5399; [PubMed: 28675200] b)Zimmermann P, Limberg C, J. Am. Chem. Soc 2017, 139, 4233–4242. [PubMed: 28170243]

[13]. a)Anderson TJ, Jones GD, Vicic DA, J. Am. Chem. Soc 2004, 126, 8100–8101; [PubMed: 15225035] b)Laskowski CA, Bungum DJ, Baldwin SM, Del Ciello SA, Iluc VM, Hillhouse

GL, J. Am. Chem. Soc 2013, 135, 18272–18275; [PubMed: 24237257] c)Kuang Y, Anthony D, Katigbak J, Marrucci F, Humagain S, Diao T, Chem 2017, 3, 268–280;d)Joannou MV, Bezdek MJ, Albahily K, Korobkov I, Chirik PJ, Organometallics 2018, 37, 3389–3393.

[14]. a)Schley ND, Fu GC, J. Am. Chem. Soc 2014, 136, 16588– 16593; [PubMed: 25402209] b)Mohadjer Beromi M, Banerjee G, Brudvig GW, Hazari N, Mercado BQ, ACS Catal. 2018, 8, 2526–2533. [PubMed: 30250755]

[15]. Kitiachvili KD, Mindiola DJ, Hillhouse GL, J. Am. Chem. Soc 2004, 126, 10554–10555. [PubMed: 15327309]

[16]. Diccianni JB, Katigbak J, Hu C, Diao T, J. Am. Chem. Soc 2019, 141, 1788–1796. [PubMed: 30612428]

[17]. Xu H, White PB, Hu C, Diao T, Angew. Chem. Int. Ed 2017, 56, 1535–1538; Angew. Chem. 2017, 129, 1557–1560.

[18]. Neese F, Wiley Interdiscip. Rev.: Comput. Mol. Sci 2012, 2, 73–78.

[19]. CCDC 1869808, 1869810, 1869811, 1916123, 1916124, 1916125, 1916126, 19161237, and 1916128 contain the supplementary crystallographic data for this paper. These data can be obtained free of charge from The Cambridge Crystallographic Data Centre.References

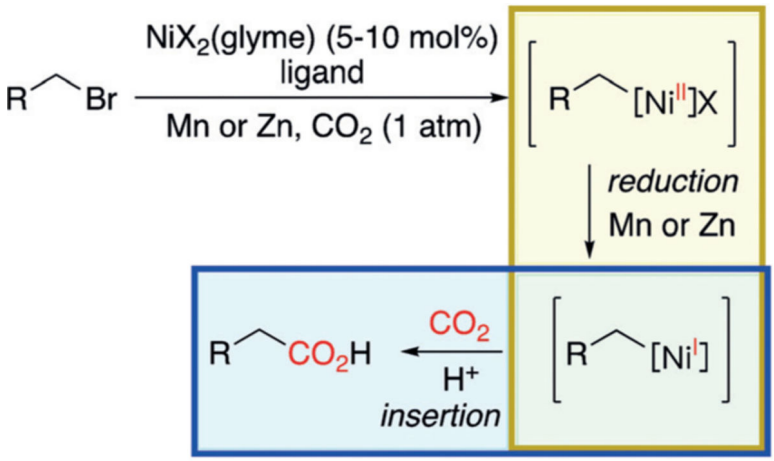

Scheme 1.

Ni-catalyzed carboxylation of an alkyl bromide via a Ni^{I}-alkyl intermediate.[4]

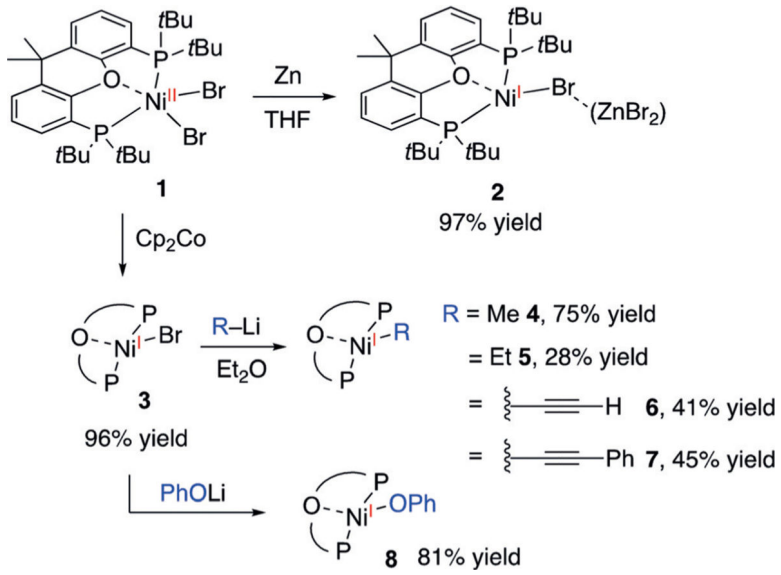

Scheme 2.

Syntheses of (*t*Bu-Xantphos)Ni-alkyl complexes and their reactivities toward CO_2. THF=tetrahydrofuran.

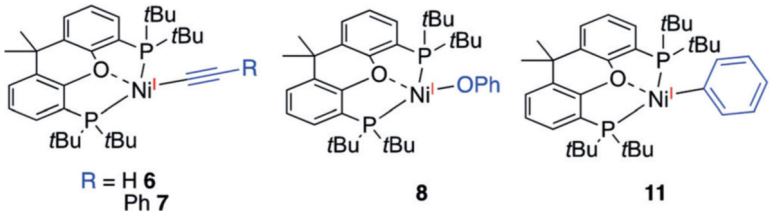

Scheme 3.

Ni^{I}-carbyl and phenoxy complexes that are unreactive toward CO_2.

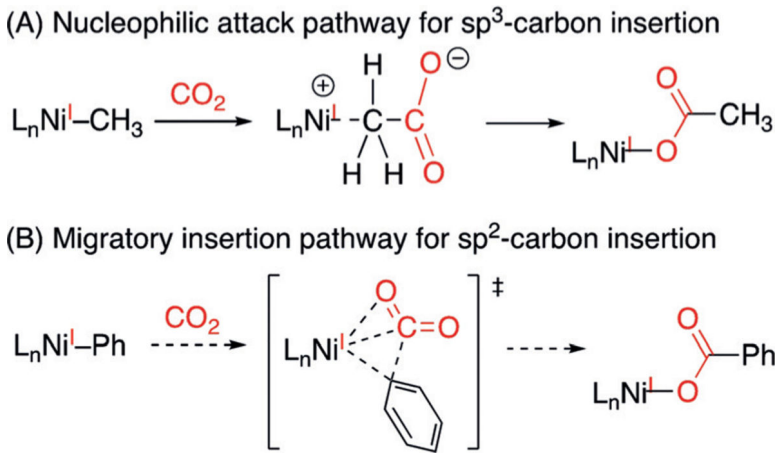

Scheme 4.
Possible pathways for Ni^{I}-mediated CO_2 insertion.

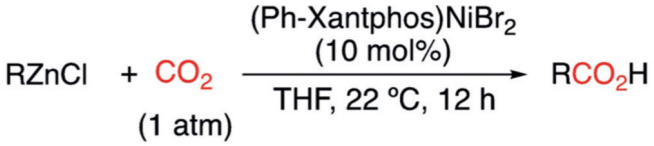

R	Yield (%)
Bn	66 (0 with no ligand)
Ph	68
n-Bu	30 (51 with (Ph-Xantphos)Ni^{I}Br)

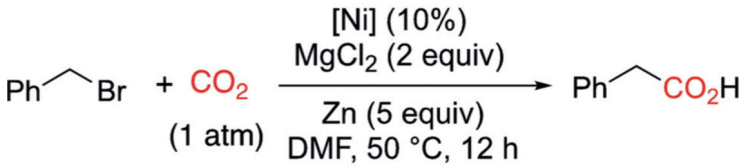

[Ni]	Yield (%)
(*t*-Bu-Xantphos)Ni^{I}Br	7
(Ph-Xantphos)Ni^{II}Br	32

Scheme 5.
(Xantphos)Ni-catalyzed carboxylation of organozinc reagents (A) and reductive carboxylation of BnBr (B). DMF=*N,N'*-dimethylformamide.

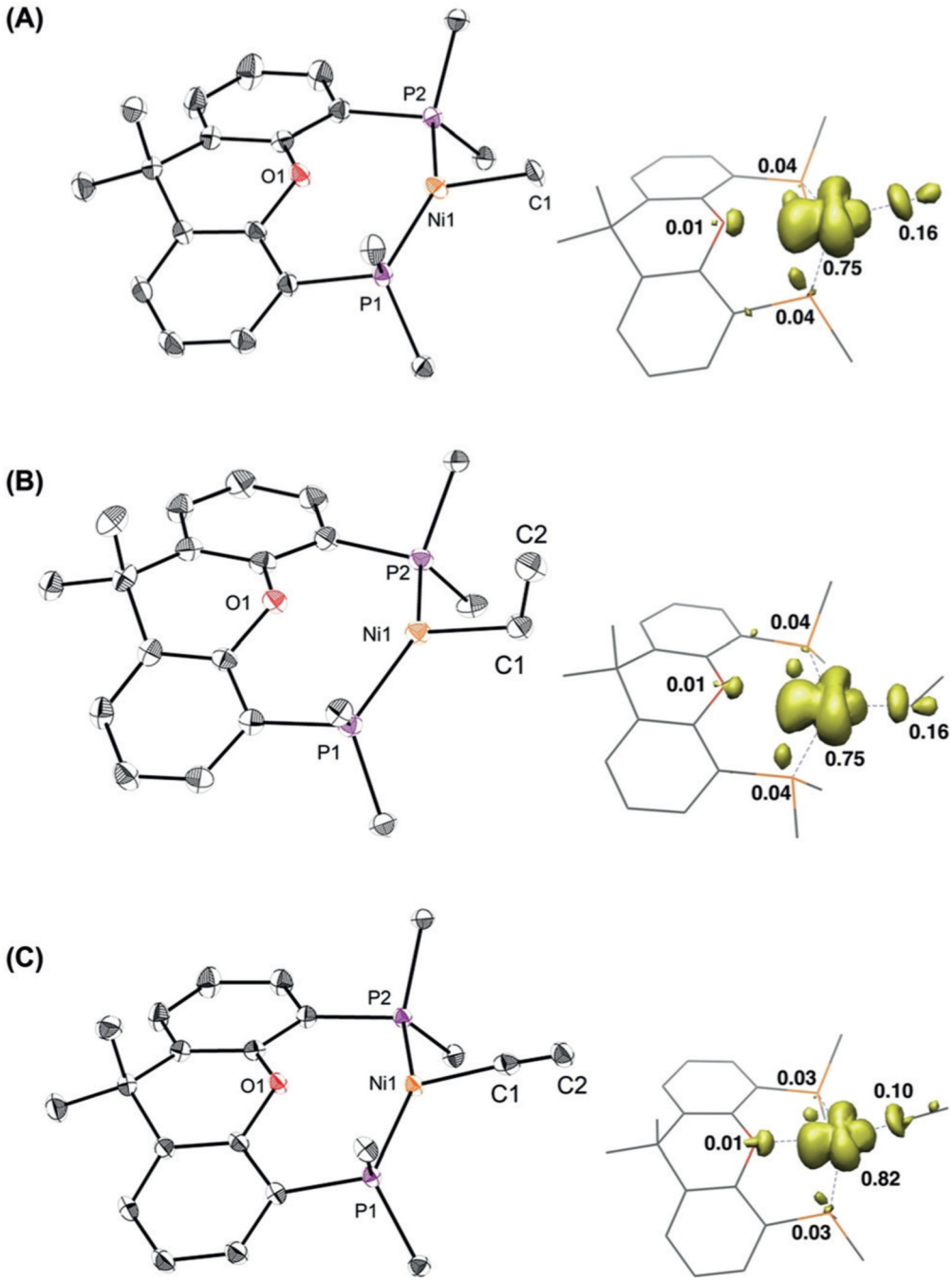

Figure 1.

X-ray structures[19] and spin-density plots of **4** (A), **5** (B), and **6** (C) at 50% probability thermal ellipsoids. Hydrogen atoms are omitted and tBu groups are truncated for clarity.

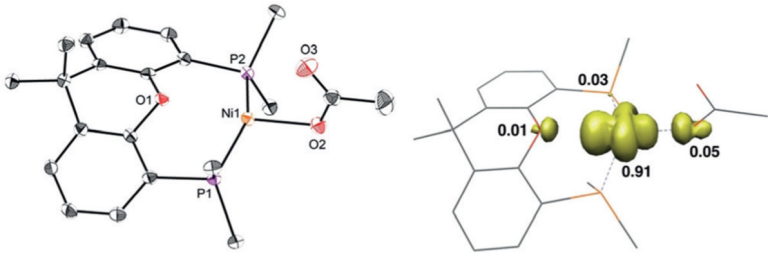

Figure 2.

X-ray structure[19] and spin-density plot of **9** at 50% probability thermal ellipsoids. Hydrogen atoms are omitted and tBu groups are truncated for clarity. Selected bond lengths [Å]: Ni(1)-O-(1)=2.0145(13), Ni(1)···O(2)=2.471, Ni(1)···O(3)=2.900.

Table 1:

Bond parameters for 4, 5, 6, and 11.

Bond length [Å] and angle [°]	**4**	**5**	**11**	**6**
C(1) hybridization	sp^3	sp^3	sp^2	sp
Ni(1)-C(1)	2.055(7)	2.034(2)	1.9795(14)	1.9359(16)
Ni(1)···O(1)	2.6018(11)	2.6737(16)	2.5184(10)	2.5405(11)
Ni(1)-C(1)-C(2)		118.07(18)		174.53(14)